

Improving the performance of twin-field quantum key distribution with advantage distillation technology

Hong-Wei Li,^{1,*} Rui-Qiang Wang,² Chun-Mei Zhang,³ and Qing-Yu Cai^{4,†}

¹Henan Key Laboratory of Quantum Information and Cryptography, SSF IEU, Zhengzhou 450000, China

²CAS Key Laboratory of Quantum Information, University of Science and Technology of China, Hefei, Anhui 230026, China

³Institute of Quantum Information and Technology,

Nanjing University of Posts and Telecommunications, Nanjing 210003, China

⁴School of Information and Communication Engineering, Hainan University, Haikou 570228, China

(Dated: March 8, 2022)

In this work, we apply two methods to improve the performance of a practical twin-field quantum key distribution system. Firstly, to improve the secure key rate, we apply the error rate in X basis, Y basis and Z basis to characterize the quantum channel. Secondly, we apply the advantage distillation method to further improve the secure key rate and transmission distance. Compared with the previous analysis result given by Maeda, Sasaki and Koashi [Nature Communication 10, 3140 (2019)], the secure key rate obtained by our analysis method will be increased at least 7%. By increasing the loss-independent misalignment error to 12%, the previous analysis method can not overcome the rate-distance bound. However, our analysis method can still overcome the rate-distance bound when the misalignment error is as large as 41%. More surprisingly, we prove that twin-field quantum key distribution can generate positive secure key even if the misalignment error is arbitrarily close to 50%, thus our analysis method can significantly improve the performance of a practical twin-field quantum key distribution system.

I. INTRODUCTION

Quantum key distribution (QKD) [1] is the art of sharing information-theoretical secure key between two different remote parties Alice and Bob. Under the perfect quantum devices preparation, the eavesdropper Eve can not get the secure key information even if she has unlimited computation and storage power [2–4]. Unfortunately, a practical QKD system is usually composed of imperfect devices, and the practical QKD system may be attacked [5–8] by utilizing imperfect quantum state preparation and measurement devices. To avoid the detector side channel attack [6, 7], measurement-device-independent QKD (MDI-QKD) protocol was proposed [9, 10]. In MDI-QKD protocol, the ideal quantum states are randomly prepared in Alice and Bob’s side, and the two quantum states will be transmitted to untrusted Charlie to apply Bell state measurement [11]. To beat the Pirandola-Laurenza-Ottaviani-Banchi (PLOB) bound [12], twin-field QKD (TF-QKD) [13] was proposed which is a variant of the MDI-QKD protocol. TF-QKD can be applied to overcome the rate scaling from η to $\sqrt{\eta}$ with a relatively simple setup, where η is the single-photon transmissivity of the link from Alice to Bob. In the TF-QKD protocol, Charlie simply conducts an interference measurement to learn the relative phase between Alice and Bob, and the secure key can be generated with in-phase and anti-phase measurement outcomes respectively. More recently, many intensive studies have been devoted to achieving information theoretic proofs of variants of TF-QKD protocols [14–19], and several practical

TF-QKD systems have been widely implemented in labs and field tests [20–26]. By applying the entanglement purification with two-way classical communication, the transmission distance of TF-QKD protocol can be improved [27].

To analyze the security of MDI-QKD protocols [9, 10], Alice and Bob should randomly prepare phase-randomized pulses in Z basis, X basis and Y basis respectively, where Z basis consists of $|0\rangle$ and $|1\rangle$, X basis consists of $|+\rangle = \frac{|0\rangle+|1\rangle}{\sqrt{2}}$ and $|-\rangle = \frac{|0\rangle-|1\rangle}{\sqrt{2}}$, and Y basis consists of $|r\rangle = \frac{|0\rangle+i|1\rangle}{\sqrt{2}}$ and $|t\rangle = \frac{|0\rangle-i|1\rangle}{\sqrt{2}}$. Note that the bit error rate in Z basis, X basis and Y basis can be applied to characterize the bit error rate and phase error rate about the quantum channel. Based on this quantum channel characterization, upper bound of the secure key information leaked to Eve can be strictly estimated. However, to estimate the bit error rate in X basis and Y basis, TF-QKD needs to generate a non-classical optical state [19, 27], which is difficult to realize in current technology. Fortunately, Maeda, Sasaki and Koashi proposed the operator dominance method [19] to estimate the bit error rate in X basis by preparing phase-randomized weak coherent state. Combining the error rate in Z basis with the error rate in X basis, the practical quantum channel in TF-QKD can be characterized, and the secure key rate can be analyzed with the entanglement distillation and purification method [2, 3, 19].

The purpose of TF-QKD is to extend the transmission distance with current technology, but the final solution is to use quantum repeater in the future research [28]. Recently, the first high-efficient and long-distance entanglement purification protocol was demonstrated [29], which shows powerful potential applications in future long-distance quantum communication. Another way to

* lihow@ustc.edu.cn

† qycail@wipm.ac.cn

extend the transmission distance is combining quantum secure direct communication with classical cryptography in a secure-repeater network framework [30].

In this work, we apply two methods to improve the performance of a practical TF-QKD system. In the first aspect, to improve the secure key rate, we apply the error rate in X basis, Y basis and Z basis to precisely characterize the practical quantum channel. By applying the information-theoretical security analysis method, we prove that the secure key rate can be improved by comparing with the previous analysis result [19]. In the second aspect, we apply advantage distillation (AD) method to further improve the secure key rate and transmission distance. AD method was initially proposed in classical cryptography theory [31], then it has been widely used in different QKD protocols [32–35] to improve the error tolerance. More recently, we analyze security of the practical BB84-QKD [1], six-state-QKD [36] and MDI-QKD [9, 10] systems by combining the AD method [4] with the decoy-state method [37–39], and the analysis results demonstrate that AD method can significantly improve the performance of different practical QKD systems [40]. Inspired by our previous work, we combine the AD method and the operator dominance method [19] to analyze security of the practical TF-QKD system, and the analysis results demonstrate that both of the transmission distance and the secure key rate can be sharply improved. More surprisingly, the analysis results also demonstrate that TF-QKD can generate positive secure key even if the loss-independent misalignment error arbitrary close to 50%, thus our analysis method can significantly improve the robustness of the practical TF-QKD system.

II. SECURITY OF QKD WITH AD

To prove security of a QKD protocol, the bit error rate of different bases should be precisely estimated. It has been proved that security of the state preparation and measurement based QKD protocol can be analyzed with the entanglement based QKD protocol [2, 4]. In the entanglement based protocol, Alice and Bob can take inputs from four-dimensional Hilbert spaces $H_A \otimes H_B$ to apply Z basis, X basis and Y basis measurements. By considering BB84 [1] and six-state [36] QKD protocols, it has been proved that Eve's general attack can be reduced to the Pauli attack [4, 41], which can be described by the classical probability theory. Thus, the QKD protocol can be illustrated with the following quantum state preparation,

$$\sigma_{AB} = \sum_{i=0}^3 \lambda_i |\Phi_i\rangle \langle \Phi_i|, \quad \text{with} \quad \sum_{i=0}^3 \lambda_i = 1, \quad (1)$$

where

$$\begin{aligned} |\Phi_0\rangle &= \frac{1}{\sqrt{2}}(|00\rangle + |11\rangle) \\ |\Phi_1\rangle &= \frac{1}{\sqrt{2}}(|00\rangle - |11\rangle) \\ |\Phi_2\rangle &= \frac{1}{\sqrt{2}}(|01\rangle + |10\rangle) \\ |\Phi_3\rangle &= \frac{1}{\sqrt{2}}(|01\rangle - |10\rangle). \end{aligned} \quad (2)$$

By combining this state preparation with the Z basis, X basis and Y basis measurement in Alice and Bob's side, the secure key rate can be given by [4]

$$\begin{aligned} R &\geq \min_{\lambda_0, \lambda_1, \lambda_2, \lambda_3} [S(A|E) - H(A|B)] \\ &= \min_{\lambda_0, \lambda_1, \lambda_2, \lambda_3} \left[1 - (\lambda_0 + \lambda_1) H\left(\frac{\lambda_0}{\lambda_0 + \lambda_1}\right) \right. \\ &\quad \left. - (\lambda_2 + \lambda_3) H\left(\frac{\lambda_2}{\lambda_2 + \lambda_3}\right) - H(\lambda_0 + \lambda_1) \right], \end{aligned} \quad (3)$$

where E is Eve's ancillary state, $S(A|E) = S(A, E) - S(E)$, $H(A|B) = H(A, B) - H(A)$, $H(x) = -x \log(x) - (1-x) \log(1-x)$ and $S(\rho) = -\text{tr}(\rho \log \rho)$ are entropy functions. Since the quantum channel can be controlled by Eve, she can choose the optimal parameters λ_i , $i = \{0, 1, 2, 3\}$ to reduce the secure key rate, but λ_i should also be restricted by the quantum bit error rate in three different bases. To analyze security of TF-QKD protocol with this information-theoretical security analysis method, we propose three virtual entanglement based QKD protocols in the following section. Since Eve cannot distinguish between entanglement based QKD protocol and prepare-and-measure QKD protocol, we can prove the security of entanglement based QKD protocol to analyze a practical TF-QKD system.

To improve the maximal tolerable error rate, the repetition code protocol based AD method has been proposed [4]. In the repetition code protocol, Alice and Bob split their raw key into blocks of b bits x_0, x_1, \dots, x_{b-1} and y_0, y_1, \dots, y_{b-1} respectively. Alice privately generates a random bit $c \in \{0, 1\}$, and sends the message $m = m_0, m_1, \dots, m_{b-1} = x_0 \oplus c, x_1 \oplus c, \dots, x_{b-1} \oplus c$ to Bob through an authenticated classical channel. Bob accepts the block if and only if $m_0 \oplus y_0, m_1 \oplus y_1, \dots, m_{b-1} \oplus y_{b-1} \in \{0, 0, \dots, 0 \text{ or } 1, 1, \dots, 1\}$. If Alice and Bob accept the block, they keep the first bit x_0 and y_0 as the raw key. Finally, Alice and Bob will apply the error correction and privacy amplification algorithms to generate the final secure key.

Based on the repetition code protocol, the secure key rate \tilde{R} can be modified as the following inequality [4]

$$\begin{aligned} \tilde{R} &\geq \max_b \min_{\lambda_0, \lambda_1, \lambda_2, \lambda_3} \frac{1}{b} p_{succ} \left[1 - (\tilde{\lambda}_0 + \tilde{\lambda}_1) H\left(\frac{\tilde{\lambda}_0}{\tilde{\lambda}_0 + \tilde{\lambda}_1}\right) \right. \\ &\quad \left. - (\tilde{\lambda}_2 + \tilde{\lambda}_3) H\left(\frac{\tilde{\lambda}_2}{\tilde{\lambda}_2 + \tilde{\lambda}_3}\right) - H(\tilde{\lambda}_0 + \tilde{\lambda}_1) \right], \end{aligned} \quad (4)$$

where

$$\begin{aligned}
\tilde{\lambda}_0 &= \frac{(\lambda_0 + \lambda_1)^b + (\lambda_0 - \lambda_1)^b}{2p_{succ}}, \\
\tilde{\lambda}_1 &= \frac{(\lambda_0 + \lambda_1)^b - (\lambda_0 - \lambda_1)^b}{2p_{succ}}, \\
\tilde{\lambda}_2 &= \frac{(\lambda_2 + \lambda_3)^b + (\lambda_2 - \lambda_3)^b}{2p_{succ}}, \\
\tilde{\lambda}_3 &= \frac{(\lambda_2 + \lambda_3)^b - (\lambda_2 - \lambda_3)^b}{2p_{succ}},
\end{aligned} \tag{5}$$

$p_{succ} = (\lambda_0 + \lambda_1)^b + (\lambda_2 + \lambda_3)^b$ is the success probability of the AD protocol. Since the AD protocol parameter b can be controlled by Alice and Bob, they can choose the optimal b to improve the secure key rate. Note that this secure key rate is based on the single photon state preparation, which can not be directly applied in the practical QKD system with weak coherent pulse or phase-randomized weak coherent pulse preparation.

III. THREE VIRTUAL PROTOCOLS TO ANALYZE THE QUANTUM CHANNEL IN TF-QKD

Based on the TF-QKD protocol proposed by Maeda, Sasaki and Koashi [19], Alice and Bob generate four different pulses with the signal state modulation and the testing state modulation respectively. In the signal state modulation, Alice and Bob randomly prepare the weak coherent pulse with amplitude $\sqrt{\mu}$ or $-\sqrt{\mu}$. In the testing state modulation, Alice and Bob randomly prepare the phase-randomized weak coherent pulse with intensities ν_1 , ν_2 and 0 respectively. For every pair of pulses received from Alice and Bob, Charlie announces whether the phase difference was successfully detected. When the phase difference was detected, Charlie further announces whether it is in-phase when detector D_1 clicks or anti-phase when detector D_2 clicks. After receiving Charlie's measurement outcomes, Alice and Bob will apply phase information on the signal state to generate the sifted key. More precisely, Charlie's measurement outcomes can be divided into two cases. In the in-phase measurement outcome case, Alice and Bob will respectively generate the random bit a with the signal state preparation $|(-1)^a \sqrt{\mu}\rangle$. In the anti-phase measurement outcome case, Alice and Bob will respectively generate the random bit a with the signal state preparation $|(-1)^a \sqrt{\mu}\rangle$ and $|(-1)^{a \oplus 1} \sqrt{\mu}\rangle$ respectively.

By applying the entanglement based protocol, the signal state preparation in Alice's side can be illustrated with the following quantum states

$$\begin{aligned}
|\psi_0\rangle_{AC_A} &= \frac{|0\rangle_A |\sqrt{\mu}\rangle_{C_A} + |1\rangle_A |-\sqrt{\mu}\rangle_{C_A}}{\sqrt{2}}, \\
|\psi_1\rangle_{AC_A} &= \frac{|0\rangle_A |\sqrt{\mu}\rangle_{C_A} - |1\rangle_A |-\sqrt{\mu}\rangle_{C_A}}{\sqrt{2}}, \\
|\psi_2\rangle_{AC_A} &= \frac{|0\rangle_A |\sqrt{\mu}\rangle_{C_A} + i|1\rangle_A |-\sqrt{\mu}\rangle_{C_A}}{\sqrt{2}}, \\
|\psi_3\rangle_{AC_A} &= \frac{|0\rangle_A |\sqrt{\mu}\rangle_{C_A} - i|1\rangle_A |-\sqrt{\mu}\rangle_{C_A}}{\sqrt{2}}.
\end{aligned} \tag{6}$$

After preparing one of the quantum states $|\psi_i\rangle_{AC_A}$, $i = \{0, 1, 2, 3\}$, Alice will measure the first quantum state, and the second quantum state will be transmitted to the quantum channel. It should be pointed out that the similar analysis method has been given in ref. [19]. Maeda, Sasaki and Koashi have proved that Alice and Bob's procedure in the signal mode can be equivalently executed by preparing the qubits AB and the optical pulses $C_A C_B$ in a joint quantum state $\frac{|0\rangle_A |\sqrt{\mu}\rangle_{C_A} + |1\rangle_A |-\sqrt{\mu}\rangle_{C_A}}{\sqrt{2}} \otimes \frac{|0\rangle_B |\sqrt{\mu}\rangle_{C_B} - |1\rangle_B |-\sqrt{\mu}\rangle_{C_B}}{\sqrt{2}}$.

By considering all of the states preparation in Eq. (6), the second quantum state ρ_{C_A} can be given by

$$\begin{aligned}
\rho_{C_A} &= tr_A |\psi_0\rangle \langle \psi_0|_{AC_A} \\
&= tr_A |\psi_1\rangle \langle \psi_1|_{AC_A} \\
&= tr_A |\psi_2\rangle \langle \psi_2|_{AC_A} \\
&= tr_A |\psi_3\rangle \langle \psi_3|_{AC_A} \\
&= \frac{1}{2} (|\sqrt{\mu}\rangle \langle \sqrt{\mu}|_{C_A} + |-\sqrt{\mu}\rangle \langle -\sqrt{\mu}|_{C_A}).
\end{aligned} \tag{7}$$

Based on this analysis result, we find that Eve can not distinguish the entanglement based protocol and the prepare-and-measure protocol. Simultaneously, the four quantum states $|\psi_i\rangle_{AC_A}$, $i = \{0, 1, 2, 3\}$ cannot be distinguished by only attacking the second quantum state, thus Eve can only apply the same operation with all of the four quantum states preparation. Similarly, the signal state preparation in Bob's side can also be illustrated with the following quantum states.

$$\begin{aligned}
|\psi_0\rangle_{BC_B} &= \frac{|0\rangle_B |\sqrt{\mu}\rangle_{C_B} + |1\rangle_B |-\sqrt{\mu}\rangle_{C_B}}{\sqrt{2}}, \\
|\psi_1\rangle_{BC_B} &= \frac{|0\rangle_B |\sqrt{\mu}\rangle_{C_B} - |1\rangle_B |-\sqrt{\mu}\rangle_{C_B}}{\sqrt{2}}, \\
|\psi_2\rangle_{BC_B} &= \frac{|0\rangle_B |\sqrt{\mu}\rangle_{C_B} + i|1\rangle_B |-\sqrt{\mu}\rangle_{C_B}}{\sqrt{2}}, \\
|\psi_3\rangle_{BC_B} &= \frac{|0\rangle_B |\sqrt{\mu}\rangle_{C_B} - i|1\rangle_B |-\sqrt{\mu}\rangle_{C_B}}{\sqrt{2}}.
\end{aligned} \tag{8}$$

To precisely estimate Eve's attacking operation in the quantum channel, we propose three virtual entanglement based protocols.

A. The first virtual protocol

In the first virtual protocol, we consider the following quantum states preparation in Alice and Bob's side

$$\begin{aligned}
\text{Alice's side : } & \frac{|0\rangle_A |\sqrt{\mu}\rangle_{C_A} + |1\rangle_A |-\sqrt{\mu}\rangle_{C_A}}{\sqrt{2}}, \\
\text{Bob's side : } & \frac{|0\rangle_B |\sqrt{\mu}\rangle_{C_B} - |1\rangle_B |-\sqrt{\mu}\rangle_{C_B}}{\sqrt{2}}.
\end{aligned} \tag{9}$$

Note that this state preparation has also been analyzed in ref. [19]. After preparing these quantum states, Alice and Bob will measure the first quantum state, and the second quantum state will be transmitted to Charlie. Thus the quantum state shared among Alice, Bob and Charlie can be given by

$$\begin{aligned}
& \frac{|0\rangle_A|\sqrt{\mu}\rangle_{C_A} + |1\rangle_A|-\sqrt{\mu}\rangle_{C_A}}{\sqrt{2}} \otimes \frac{|0\rangle_B|\sqrt{\mu}\rangle_{C_B} - |1\rangle_B|-\sqrt{\mu}\rangle_{C_B}}{\sqrt{2}} \\
&= \frac{1}{4}[(|0\rangle|0\rangle + |1\rangle|1\rangle)_{AB}(|\sqrt{\mu}\rangle|\sqrt{\mu}\rangle - |-\sqrt{\mu}\rangle|-\sqrt{\mu}\rangle)_{C_A,C_B} \\
&+ (|0\rangle|0\rangle - |1\rangle|1\rangle)_{AB}(|\sqrt{\mu}\rangle|\sqrt{\mu}\rangle + |-\sqrt{\mu}\rangle|-\sqrt{\mu}\rangle)_{C_A,C_B} \\
&+ (|0\rangle|1\rangle + |1\rangle|0\rangle)_{AB}(-|\sqrt{\mu}\rangle|-\sqrt{\mu}\rangle + |-\sqrt{\mu}\rangle|\sqrt{\mu}\rangle)_{C_A,C_B} \\
&+ (|0\rangle|1\rangle - |1\rangle|0\rangle)_{AB}(-|\sqrt{\mu}\rangle|-\sqrt{\mu}\rangle - |-\sqrt{\mu}\rangle|\sqrt{\mu}\rangle)_{C_A,C_B}]. \tag{10}
\end{aligned}$$

After measuring the received quantum states C_A and C_B with a 50 : 50 beam-splitter and a pair of photon detectors D_1 and D_2 , Charlie announces whether the phase difference is successfully detected, and this quantum state will be transformed to

$$\begin{aligned}
& \frac{1}{4}[(|0\rangle|0\rangle + |1\rangle|1\rangle)_{AB}(|\sqrt{2\mu}\rangle|0\rangle - |-\sqrt{2\mu}\rangle|0\rangle)_{D_1,D_2} + \\
& (|0\rangle|0\rangle - |1\rangle|1\rangle)_{AB}(|\sqrt{2\mu}\rangle|0\rangle + |-\sqrt{2\mu}\rangle|0\rangle)_{D_1,D_2} + \\
& (|0\rangle|1\rangle + |1\rangle|0\rangle)_{AB}(-|0\rangle|\sqrt{2\mu}\rangle + |0\rangle|-\sqrt{2\mu}\rangle)_{D_1,D_2} + \\
& (|0\rangle|1\rangle - |1\rangle|0\rangle)_{AB}(-|0\rangle|\sqrt{2\mu}\rangle - |0\rangle|-\sqrt{2\mu}\rangle)_{D_1,D_2}], \tag{11}
\end{aligned}$$

where the detection results that detector D_1 clicks and detector D_2 clicks respectively demonstrate the in-phase and anti-phase measurement outcomes in Charlie's side. Here, for the simplicity of the discussion, we assume that they are no channel losses. Correspondingly, the quantum states $(|\sqrt{2\mu}\rangle|0\rangle - |-\sqrt{2\mu}\rangle|0\rangle)_{D_1,D_2}$ and $(|\sqrt{2\mu}\rangle|0\rangle + |-\sqrt{2\mu}\rangle|0\rangle)_{D_1,D_2}$ demonstrate the in-phase measurement outcome, while quantum states $(-|0\rangle|\sqrt{2\mu}\rangle + |0\rangle|-\sqrt{2\mu}\rangle)_{D_1,D_2}$ and $(-|0\rangle|\sqrt{2\mu}\rangle - |0\rangle|-\sqrt{2\mu}\rangle)_{D_1,D_2}$ demonstrate the anti-phase measurement outcome. Note that TF-QKD protocol is a variant of the MDI-QKD protocol, thus the measurement outcomes can be assumed to be controlled by Eve. We can simply assume the click of detector D_1 demonstrates the Bell state $\frac{1}{\sqrt{2}}(|0\rangle|0\rangle + |1\rangle|1\rangle)_{AB}$ preparation in Alice and Bob's side, while the click of detector D_2 demonstrates the Bell state $\frac{1}{\sqrt{2}}(|0\rangle|1\rangle + |1\rangle|0\rangle)_{AB}$ preparation in Alice and Bob's side. Since Charlie's measurement outcomes have no security requirement, this assumption is reasonable, and more detailed explanation has been given in ref. [19].

By applying the time reversed entanglement technique, we can assume the Bell states $\frac{1}{\sqrt{2}}(|0\rangle|0\rangle + |1\rangle|1\rangle)_{AB}$ and $\frac{1}{\sqrt{2}}(|0\rangle|1\rangle + |1\rangle|0\rangle)_{AB}$ is prepared in Charlie's side, then the two quantum states will be transmitted to Alice and Bob to perform Z basis or X basis measurement. Based on this analysis method, the in-phase measurement outcome demonstrates the Bell state preparation

$$\frac{1}{\sqrt{2}}(|0\rangle|0\rangle + |1\rangle|1\rangle)_{AB} = \frac{1}{\sqrt{2}}(|+\rangle|+\rangle + |-\rangle|-\rangle)_{AB}. \tag{12}$$

Suppose Alice and Bob apply Z basis measurement, Z basis error is defined to be an event where the pair is found in either state $|0\rangle|1\rangle_{AB}$ or $|1\rangle|0\rangle_{AB}$. Suppose Alice and Bob apply X basis measurement, X basis error is defined to be an event where the pair is found in either state $|+\rangle|-\rangle_{AB}$ or $|-\rangle|+\rangle_{AB}$.

Similarly, the anti-phase measurement outcome

demonstrates the Bell state preparation

$$\frac{1}{\sqrt{2}}(|0\rangle|1\rangle + |1\rangle|0\rangle)_{AB} = \frac{1}{\sqrt{2}}(|+\rangle|+\rangle - |-\rangle|-\rangle)_{AB}. \tag{13}$$

Suppose Alice and Bob apply Z basis measurement, Z basis error is defined to be an event where the pair was found in either state $|0\rangle|0\rangle_{AB}$ or $|1\rangle|1\rangle_{AB}$. Suppose Alice and Bob apply X basis measurement, X basis error is defined to be an event where the pair is found in either state $|+\rangle|-\rangle_{AB}$ or $|-\rangle|+\rangle_{AB}$.

In a practical TF-QKD experiment, the bit error rate in Z basis can be directly tested, but the bit error rate in X basis and Y basis can not be directly observed. To analyze the bit error rate in X basis, the quantum state shared among Alice, Bob and Charlie can be rewritten as

$$\begin{aligned}
& \frac{|0\rangle_A|\sqrt{\mu}\rangle_{C_A} + |1\rangle_A|-\sqrt{\mu}\rangle_{C_A}}{\sqrt{2}} \otimes \frac{|0\rangle_B|\sqrt{\mu}\rangle_{C_B} - |1\rangle_B|-\sqrt{\mu}\rangle_{C_B}}{\sqrt{2}} \\
&= \sqrt{c_+}|+\rangle_A|\sqrt{\mu_{\text{even}}}\rangle_{C_A} + \sqrt{c_-}|-\rangle_A|\sqrt{\mu_{\text{odd}}}\rangle_{C_A} \\
&\otimes (\sqrt{c_-}|+\rangle_B|\sqrt{\mu_{\text{odd}}}\rangle_{C_B} + \sqrt{c_+}|-\rangle_B|\sqrt{\mu_{\text{even}}}\rangle_{C_B}), \tag{14}
\end{aligned}$$

where $c_+ := e^{-\mu} \cosh \mu$, $c_- := e^{-\mu} \sinh \mu$, $|\sqrt{\mu_{\text{even}}}\rangle = (|\sqrt{\mu}\rangle + |-\sqrt{\mu}\rangle)/2\sqrt{c_+}$ and $|\sqrt{\mu_{\text{odd}}}\rangle = (|\sqrt{\mu}\rangle - |-\sqrt{\mu}\rangle)/2\sqrt{c_-}$. Based on this state preparation, the X basis error occurs with probability $p_{\text{even}} = c_+^2 + c_-^2 = e^{-2\mu} \cosh 2\mu$, and the optical pulses are sent in the following quantum state

$$\begin{aligned}
p_{\text{even}} \rho^{\text{even}} = & c_+^2 |\sqrt{\mu_{\text{even}}}\sqrt{\mu_{\text{even}}}\rangle \langle \sqrt{\mu_{\text{even}}}\sqrt{\mu_{\text{even}}}|_{C_A C_B} \\
& + c_-^2 |\sqrt{\mu_{\text{odd}}}\sqrt{\mu_{\text{odd}}}\rangle \langle \sqrt{\mu_{\text{odd}}}\sqrt{\mu_{\text{odd}}}|_{C_A C_B}. \tag{15}
\end{aligned}$$

To analyze the error rate in X basis, the counting rate with this non-classical optical state preparation can be analyzed with the operator dominance method [19], where the detection frequency of ρ^{even} can be estimated from a combination of phase-randomized weak coherent states with intensities ν_1 , ν_2 and 0. More detailed explanation has been given in the methods section in ref. [19].

B. The second virtual protocol

In the second virtual protocol, we consider the following quantum state preparation in Alice and Bob's side

$$\begin{aligned}
\text{Alice's side : } & \frac{|0\rangle_A|\sqrt{\mu}\rangle_{C_A} + i|1\rangle_A|-\sqrt{\mu}\rangle_{C_A}}{\sqrt{2}}, \\
\text{Bob's side : } & \frac{|0\rangle_B|\sqrt{\mu}\rangle_{C_B} + i|1\rangle_B|-\sqrt{\mu}\rangle_{C_B}}{\sqrt{2}}. \tag{16}
\end{aligned}$$

Based on this state preparation, the quantum state shared among Alice, Bob and Charlie can be given by

$$\begin{aligned}
& \frac{|0\rangle_A|\sqrt{\mu}\rangle_{C_A} + i|1\rangle_A|-\sqrt{\mu}\rangle_{C_A}}{\sqrt{2}} \otimes \frac{|0\rangle_B|\sqrt{\mu}\rangle_{C_B} + i|1\rangle_B|-\sqrt{\mu}\rangle_{C_B}}{\sqrt{2}} \\
&= \frac{1}{4}[(|0\rangle|0\rangle + |1\rangle|1\rangle)_{AB}(|\sqrt{\mu}\rangle|\sqrt{\mu}\rangle - |-\sqrt{\mu}\rangle|-\sqrt{\mu}\rangle)_{C_A C_B} \\
&+ (|0\rangle|0\rangle - |1\rangle|1\rangle)_{AB}(|\sqrt{\mu}\rangle|\sqrt{\mu}\rangle + |-\sqrt{\mu}\rangle|-\sqrt{\mu}\rangle)_{C_A C_B} \\
&+ (|0\rangle|1\rangle + |1\rangle|0\rangle)_{AB}(i|\sqrt{\mu}\rangle|-\sqrt{\mu}\rangle + i|-\sqrt{\mu}\rangle|\sqrt{\mu}\rangle)_{C_A C_B} \\
&+ (|0\rangle|1\rangle - |1\rangle|0\rangle)_{AB}(i|\sqrt{\mu}\rangle|-\sqrt{\mu}\rangle - i|-\sqrt{\mu}\rangle|\sqrt{\mu}\rangle)_{C_A C_B}]. \tag{17}
\end{aligned}$$

After measuring the received quantum states C_A and C_B , Charlie announces whether the phase difference was successfully detected, and this quantum state will be transformed to

$$\begin{aligned} & \frac{1}{4}[(|0\rangle|0\rangle + |1\rangle|1\rangle)_{AB}(|\sqrt{2\mu}\rangle|0\rangle - |-\sqrt{2\mu}\rangle|0\rangle)_{D_1D_2} \\ & + (|0\rangle|0\rangle - |1\rangle|1\rangle)_{AB}(|\sqrt{2\mu}\rangle|0\rangle + |-\sqrt{2\mu}\rangle|0\rangle)_{D_1D_2} \\ & + (|0\rangle|1\rangle + |1\rangle|0\rangle)_{AB}(i|0\rangle|\sqrt{2\mu}\rangle + i|0\rangle|-\sqrt{2\mu}\rangle)_{D_1D_2} \\ & + (|0\rangle|1\rangle - |1\rangle|0\rangle)_{AB}(i|0\rangle|\sqrt{2\mu}\rangle - i|0\rangle|-\sqrt{2\mu}\rangle)_{D_1D_2}]. \end{aligned} \quad (18)$$

Note that the quantum states $(|\sqrt{2\mu}\rangle|0\rangle - |-\sqrt{2\mu}\rangle|0\rangle)_{D_1D_2}$ and $(|\sqrt{2\mu}\rangle|0\rangle + |-\sqrt{2\mu}\rangle|0\rangle)_{D_1D_2}$ demonstrate the in-phase measurement outcome. Since the detection result can be controlled by Eve, we can simply assume the click of detector D_1 demonstrates the Bell state $\frac{1}{\sqrt{2}}(|0\rangle|0\rangle + |1\rangle|1\rangle)_{AB}$ preparation in Alice and Bob's side. By applying the time reversed entanglement technique, we assume the Bell state $\frac{1}{\sqrt{2}}(|0\rangle|0\rangle + |1\rangle|1\rangle)_{AB}$ is prepared in Charlie's side, then the two quantum states will be transmitted to Alice and Bob to perform Z basis or Y basis measurements. Based on this analysis method, the in-phase measurement outcome demonstrates the following Bell state preparation

$$\frac{1}{\sqrt{2}}(|0\rangle|0\rangle + |1\rangle|1\rangle)_{AB} = \frac{1}{\sqrt{2}}(|r\rangle|t\rangle + |t\rangle|r\rangle)_{AB}. \quad (19)$$

Suppose Alice and Bob apply Y basis measurement, Y basis error is defined to be an event where the pair is found in either state $|r\rangle|r\rangle$ or $|t\rangle|t\rangle$. To analyze the bit error rate in Y basis with the Bell state $\frac{1}{\sqrt{2}}(|0\rangle|0\rangle + |1\rangle|1\rangle)_{AB}$ preparation, the quantum state shared among Alice, Bob and Charlie can be rewritten as

$$\begin{aligned} & \frac{|0\rangle_A|\sqrt{\mu}\rangle_{C_A} + i|1\rangle_A|-\sqrt{\mu}\rangle_{C_A}}{\sqrt{2}} \otimes \frac{|0\rangle_B|\sqrt{\mu}\rangle_{C_B} + i|1\rangle_B|-\sqrt{\mu}\rangle_{C_B}}{\sqrt{2}} \\ & = (\sqrt{c_+}|r\rangle_A|\sqrt{\mu_{even}}\rangle_{C_A} + \sqrt{c_-}|t\rangle_A|\sqrt{\mu_{odd}}\rangle_{C_A}) \\ & \otimes (\sqrt{c_+}|r\rangle_B|\sqrt{\mu_{even}}\rangle_{C_B} + \sqrt{c_-}|t\rangle_B|\sqrt{\mu_{odd}}\rangle_{C_B}). \end{aligned} \quad (20)$$

Based on this state preparation, we can interpret that the Y basis error occurs with probability p_{even} and the optical pulses are sent in state ρ^{even} .

By considering the first and second virtual protocols, we can prove that Eq. (14) is equal to Eq. (20). Since Eve cannot distinguish Eqs. (14) and (20), she can only apply the same operation in the quantum channel. Thus, the error rate in X basis is equal to the error rate in Y basis if Alice and Bob prepare the Bell state $\frac{1}{\sqrt{2}}(|0\rangle|0\rangle + |1\rangle|1\rangle)_{AB}$.

C. The third virtual protocol

In the third virtual protocol, we consider the following quantum state preparation

$$\begin{aligned} \text{Alice's side : } & \frac{|0\rangle_A|\sqrt{\mu}\rangle_{C_A} + i|1\rangle_A|-\sqrt{\mu}\rangle_{C_A}}{\sqrt{2}}, \\ \text{Bob's side : } & \frac{|0\rangle_B|\sqrt{\mu}\rangle_{C_B} - i|1\rangle_B|-\sqrt{\mu}\rangle_{C_B}}{\sqrt{2}}. \end{aligned} \quad (21)$$

The quantum state shared among Alice, Bob and Charlie can be given by

$$\begin{aligned} & \frac{|0\rangle_A|\sqrt{\mu}\rangle_{C_A} + i|1\rangle_A|-\sqrt{\mu}\rangle_{C_A}}{\sqrt{2}} \otimes \frac{|0\rangle_B|\sqrt{\mu}\rangle_{C_B} - i|1\rangle_B|-\sqrt{\mu}\rangle_{C_B}}{\sqrt{2}} \\ & = \frac{1}{4}[(|0\rangle|0\rangle + |1\rangle|1\rangle)_{AB}(|\sqrt{\mu}\rangle|\sqrt{\mu}\rangle + |-\sqrt{\mu}\rangle|-\sqrt{\mu}\rangle)_{C_AC_B} \\ & + (|0\rangle|0\rangle - |1\rangle|1\rangle)_{AB}(|\sqrt{\mu}\rangle|\sqrt{\mu}\rangle - |-\sqrt{\mu}\rangle|-\sqrt{\mu}\rangle)_{C_AC_B} \\ & + (|0\rangle|1\rangle + |1\rangle|0\rangle)_{AB}(-i|\sqrt{\mu}\rangle|-\sqrt{\mu}\rangle + i|-\sqrt{\mu}\rangle|\sqrt{\mu}\rangle)_{C_AC_B} \\ & + (|0\rangle|1\rangle - |1\rangle|0\rangle)_{AB}(-i|\sqrt{\mu}\rangle|-\sqrt{\mu}\rangle - i|-\sqrt{\mu}\rangle|\sqrt{\mu}\rangle)_{C_AC_B}]. \end{aligned} \quad (22)$$

After measuring the received quantum states C_A and C_B , Charlie announces whether the phase difference is successfully detected, and the quantum state will be transformed to

$$\begin{aligned} & \frac{1}{4}[(|0\rangle|0\rangle + |1\rangle|1\rangle)_{AB}(|\sqrt{2\mu}\rangle|0\rangle + |-\sqrt{2\mu}\rangle|0\rangle)_{D_1D_2} \\ & + (|0\rangle|0\rangle - |1\rangle|1\rangle)_{AB}(|\sqrt{2\mu}\rangle|0\rangle - |-\sqrt{2\mu}\rangle|0\rangle)_{D_1D_2} \\ & + (|0\rangle|1\rangle + |1\rangle|0\rangle)_{AB}(-i|0\rangle|\sqrt{2\mu}\rangle + i|0\rangle|-\sqrt{2\mu}\rangle)_{D_1D_2} \\ & + (|0\rangle|1\rangle - |1\rangle|0\rangle)_{AB}(-i|0\rangle|\sqrt{2\mu}\rangle - i|0\rangle|-\sqrt{2\mu}\rangle)_{D_1D_2}]. \end{aligned} \quad (23)$$

Note that the quantum states $(-i|0\rangle|\sqrt{2\mu}\rangle + i|0\rangle|-\sqrt{2\mu}\rangle)_{D_1D_2}$ and $(-i|0\rangle|\sqrt{2\mu}\rangle - i|0\rangle|-\sqrt{2\mu}\rangle)_{D_1D_2}$ demonstrate the anti-phase measurement outcome. Since the detection result can be controlled by Eve, we can simply assume the click of detector D_2 demonstrates the Bell state $\frac{1}{\sqrt{2}}(|0\rangle|1\rangle + |1\rangle|0\rangle)_{AB}$ preparation in Alice and Bob's side. By applying the time reversed entanglement technique, we assume the Bell state $\frac{1}{\sqrt{2}}(|0\rangle|1\rangle + |1\rangle|0\rangle)_{AB}$ is prepared in Charlie's side, then the two quantum states will be transmitted to Alice and Bob to perform Z basis or Y basis measurements. Based on this analysis method, the anti-phase measurement outcome demonstrates the Bell state preparation

$$\frac{1}{\sqrt{2}}(|0\rangle|1\rangle + |1\rangle|0\rangle)_{AB} = \frac{-i}{\sqrt{2}}(|r\rangle|r\rangle - |t\rangle|t\rangle)_{AB}. \quad (24)$$

Suppose Alice and Bob apply Y basis measurement, Y basis error is defined to be an event where the pair is found in either state $|r\rangle|t\rangle$ or $|t\rangle|r\rangle$. To analyze the bit error rate in Y basis with Bell state $\frac{1}{\sqrt{2}}(|0\rangle|1\rangle + |1\rangle|0\rangle)_{AB}$ preparation, the quantum state shared among Alice, Bob and Charlie can be rewritten as

$$\begin{aligned} & \frac{|0\rangle_A|\sqrt{\mu}\rangle_{C_A} + i|1\rangle_A|-\sqrt{\mu}\rangle_{C_A}}{\sqrt{2}} \otimes \frac{|0\rangle_B|\sqrt{\mu}\rangle_{C_B} - i|1\rangle_B|-\sqrt{\mu}\rangle_{C_B}}{\sqrt{2}} \\ & = (\sqrt{c_+}|r\rangle_A|\sqrt{\mu_{even}}\rangle_{C_A} + \sqrt{c_-}|t\rangle_A|\sqrt{\mu_{odd}}\rangle_{C_A}) \\ & \otimes (\sqrt{c_-}|r\rangle_B|\sqrt{\mu_{odd}}\rangle_{C_B} + \sqrt{c_+}|t\rangle_B|\sqrt{\mu_{even}}\rangle_{C_B}) \end{aligned} \quad (25)$$

Based on this state preparation, we can interpret that Y basis error occurs with probability p_{even} and the optical pulses are sent in state ρ^{even} .

By considering the first and third virtual protocols, we can prove that Eq. (14) is equal to Eq. (25). Since Eve cannot distinguish Eqs. (14) and (25), she can only apply the same operation in the quantum channel. Thus, the error rate in X basis is equal to the error rate in Y basis if Alice and Bob prepare the Bell state $\frac{1}{\sqrt{2}}(|0\rangle|1\rangle + |1\rangle|0\rangle)_{AB}$.

Combining with these three virtual protocols, we can prove that the error rate in X basis is equal to the error rate in Y basis no matter Alice and Bob prepare the

Bell state $\frac{1}{\sqrt{2}}(|0\rangle|0\rangle + |1\rangle|1\rangle)_{AB}$ or $\frac{1}{\sqrt{2}}(|0\rangle|1\rangle + |1\rangle|0\rangle)_{AB}$. Combining this analysis result with the operator dominance method given by [19], we can precisely estimate the quantum channel parameters λ_i , $i = \{0, 1, 2, 3\}$ in the following section.

IV. SECURITY OF TF-QKD WITH AD

By applying the previous analysis result with the signal state modulation in Alice and Bob's side, we need to analyze the error rate E_{uu}^{ZZ} in Z basis, the error rate E_{uu}^{XX} in X basis and the error rate E_{uu}^{YY} in Y basis respectively. In a practical TF-QKD experiment, E_{uu}^{ZZ} can be directly calculated by testing part of the in-phase and anti-phase measurement outcomes. However, the non-classical optical state ρ^{even} is hard to realize in current technology, the bit error rate E_{uu}^{XX} and E_{uu}^{YY} can not be directly estimated in a practical TF-QKD system. Fortunately, Maeda, Sasaki and Koashi proposed the operator dominance method to estimate E_{uu}^{XX} [19], where the number of testing states forming the linear combination to approximate the non-classical optical state ρ^{even} . In the previous section, we prove that $E_{uu}^{XX} = E_{uu}^{ZZ}$, thus the practical quantum channel can be characterized with E_{uu}^{XX} , E_{uu}^{YY} and E_{uu}^{ZZ} . To analyze the security of the entanglement based TF-QKD protocol with the information-theoretical analysis method, the relationship among E_{uu}^{ZZ} , E_{uu}^{XX} , E_{uu}^{YY} and λ_i can be given with the following equations,

$$\begin{aligned}\lambda_1 + \lambda_3 &= E_{uu}^{XX}, \\ \lambda_2 + \lambda_3 &= E_{uu}^{ZZ}, \\ \lambda_1 + \lambda_2 &= E_{uu}^{YY},\end{aligned}\quad (26)$$

where $\lambda_0 + \lambda_1 + \lambda_2 + \lambda_3 = 1$. Based on these equations, all of the quantum channel parameters λ_i , $i = \{0, 1, 2, 3\}$ can be accurately solved.

In the TF-QKD protocol, only the signal state can be used to generate the final secure key. Since the quantum channel parameters can be solved in Eq. (26), Eq. (4) can be modified with the following inequality by applying the AD method

$$\begin{aligned}R_{TF} &\geq \max_b \frac{1}{b} q_{succ}^{ZZ} Q_{uu}^{ZZ} [S(A|E) - H(A|B)] \\ &= \max_b \frac{1}{b} q_{succ}^{ZZ} Q_{uu}^{ZZ} [(1 - (\tilde{\lambda}_0 + \tilde{\lambda}_1))H(\frac{\tilde{\lambda}_0}{\tilde{\lambda}_0 + \tilde{\lambda}_1}) \\ &\quad - (\tilde{\lambda}_2 + \tilde{\lambda}_3)H(\frac{\tilde{\lambda}_2}{\tilde{\lambda}_2 + \tilde{\lambda}_3}) - fh(E_{uu}^{ZZ})],\end{aligned}\quad (27)$$

where Q_{uu}^{ZZ} is the counting rate by considering Alice and Bob prepare the signal states, $E_{uu}^{ZZ} = \frac{E_{uu}^{ZZ^b}}{E_{uu}^{ZZ^b} + (1 - E_{uu}^{ZZ})^b}$ is the error rate after the AD protocol, $f > 1$ is the error correction efficiency, $q_{succ}^{ZZ} = E_{uu}^{ZZ^b} + (1 - E_{uu}^{ZZ})^b$ is the successful probability of the AD method in the practical TF-QKD system.

By applying the operator dominance method with asymptotic key length, the error rate in X basis $E_{\mu\mu}^{XX}$ and the error rate in Y basis $E_{\mu\mu}^{YY}$ can be given by [19]

$$E_{\mu\mu}^{XX} = E_{\mu\mu}^{YY} = C_1(1 + \sqrt{(C_2 + C_4)C_3})^2, \quad (28)$$

where $C_1 = \frac{e^{-2\mu}d}{1 - e^{-2\mu\eta} + e^{-2\mu\eta}d}$, $C_2 = \frac{e^{-2\nu_1(\nu_1 - \nu_2)}}{\mu_2}$, $C_3 = \frac{1}{\nu_1 e^{-2\nu_1}} \sum_{k=1}^{\infty} \frac{\mu^{2k}(k+1)}{\nu_1^{2k-1} - \nu_2^{2k-1}}$, $C_4 = \frac{1}{d}(1 - e^{-2\nu_1\eta} + e^{-2\nu_1\eta}d - \frac{\nu_1 e^{-2\nu_1}}{\nu_2 e^{-2\nu_2}}(1 - e^{-2\nu_2\eta} + e^{-2\nu_2\eta}d))$, $\max(\mu, \nu_2) < \nu_1$. Note that, we assume each detector has a dark count probability of p_d , which amounts to the effective probability $d = 2p_d - p_d^2$ from the two detectors. By considering the channel transmission efficiency, the overall transmissivity from Alice (Bob) to Charlie's detection is η .

Based on the simulation parameters given by [19], we calculate the secure key rate R_{TF} as a function of secure key rate transmission distance L between Alice and Bob. We assume a fiber loss of 0.2 dB/km, a loss-independent misalignment error of $e_d = 0.03$, error correction efficiency $f = 1.1$, each detector has a detection efficiency $\eta_d = 0.3$ and dark count probability $p_d = 10^{-8}$. The overall transmissivity from Alice (Bob) to Charlie's detection is then $\eta = \eta_d 10^{-0.01L}$. In the asymptotic limit, the counting rate of Alice and Bob's signal states Q_{uu}^{ZZ} can be given by

$$Q_{uu}^{ZZ} = 1 - e^{-2\mu\eta} + e^{-2\mu\eta}d, \quad (29)$$

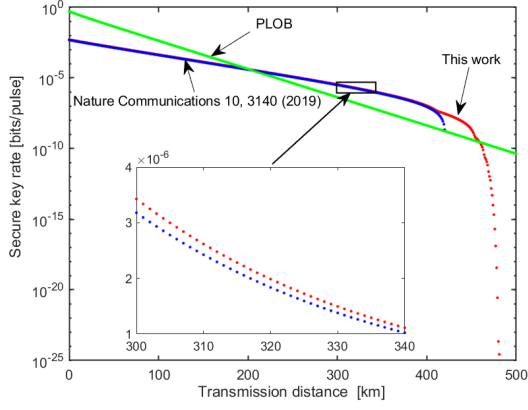
Correspondingly, the error rate in Z basis $E_{\mu\mu}^{ZZ}$ can be given by

$$E_{\mu\mu}^{ZZ} = \frac{e_d(1 - e^{-2\mu\eta}) + e^{-2\mu\eta}d}{Q_{uu}^{ZZ}}. \quad (30)$$

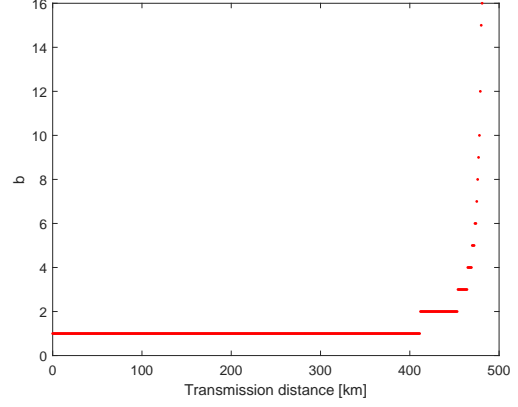
Based on these simulation parameters and the optimal b values, we calculate the secure key rate R_{TF} as a function of transmission distance between Alice and Bob in Figure 1. By comparing with the previous analysis result given by [19], we find that both of the two analysis results can overcome the PLOB bound $-\log(1 - \eta_d 10^{-0.02L})$, but our analysis method can generate the secure key rate at least 7% higher than the previous method even without utilizing the AD method. By applying the AD method, the simulation result demonstrates that the maximal secure key transmission distance can be significantly improved from 430 km to 480 km.

By increasing the loss-independent misalignment error to $e_d = 0.12$, we calculate the secure key rate in Figure 2. We find that our analysis result can overcome the PLOB bound, but the secure key rate with the previous analysis method can not overcome the PLOB bound at any transmission distance. The secure key rate obtained by our method is at least 1.5 times higher than that of the original method, and the maximal secure key transmission distance can be improved from 345 km to 466 km.

By increasing the loss-independent misalignment error to $e_d = 0.3$, we calculate the secure key rate in Figure

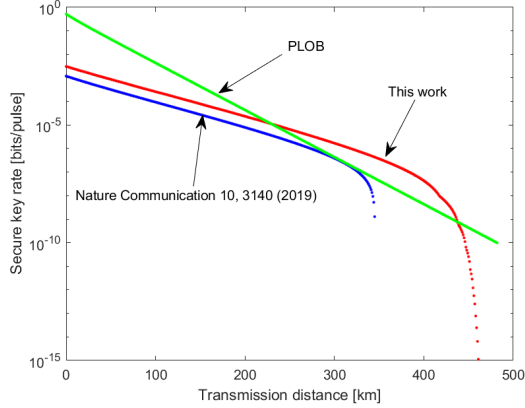


(a) The relationship between the transmission distance and the secure key rate, the blue line is the secure key rate given by [19], the red line is the secure key rate given by this work, and the green line is the PLOB bound.

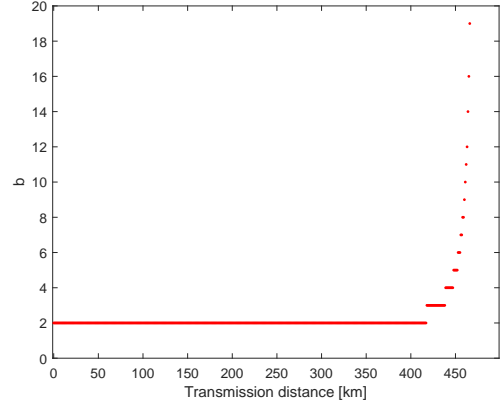


(b) The relationship between the transmission distance and the optimal b values. From 0 km to 411 km, the optimal b value is 1, thus we do not need to utilize the AD method in these transmission distances.

FIG. 1. Results of TF-QKD protocol with $e_d = 0.03$.



(a) The relationship between the transmission distance and the secure key rate, the blue line is the secret key rate given by [19], the red line is the secure key rate given by this work, and the green line is the PLOB bound.



(b) The relationship between the transmission distance and the optimal b values. From 0 km to 417 km, the optimal b value is 2.

FIG. 2. Results of TF-QKD protocol with $e_d = 0.12$.

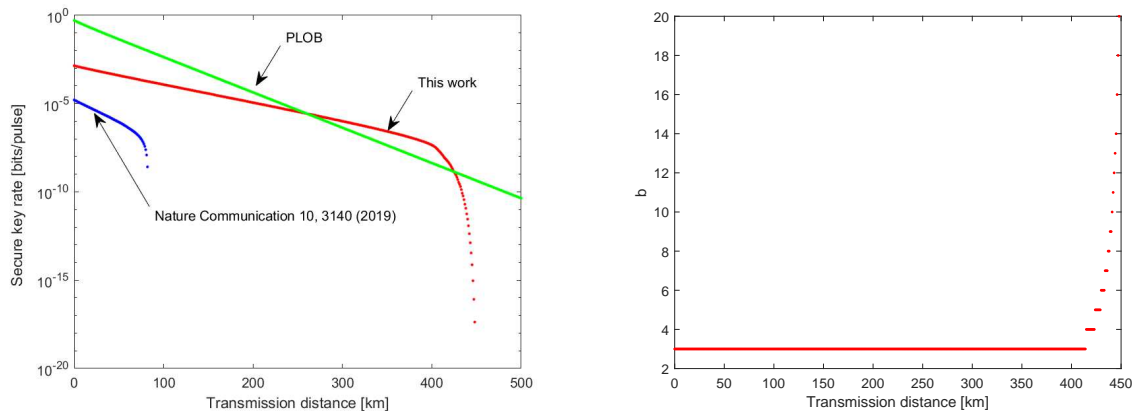
3. We find that the secure key rate obtained by our method is at least 85 times higher than that of the original method, and the maximal secure key transmission distance can be sharply improved from 82 km to 448 km.

By increasing the loss-independent misalignment error to $e_d = 0.41$, we calculate the secure key rate in Figure 4. We find that our analysis result can still overcome the PLOB bound, and the maximal secure key transmission distance can also be reached to 448 km. But the previous analysis method can not generate positive secure key rate even at 0 km transmission distance.

By increasing the loss-independent misalignment error to $e_d = 0.49$, we calculate the secure key rate in Figure 5. More surprisingly, our simulation result demonstrates that the maximal secure key transmission distance can

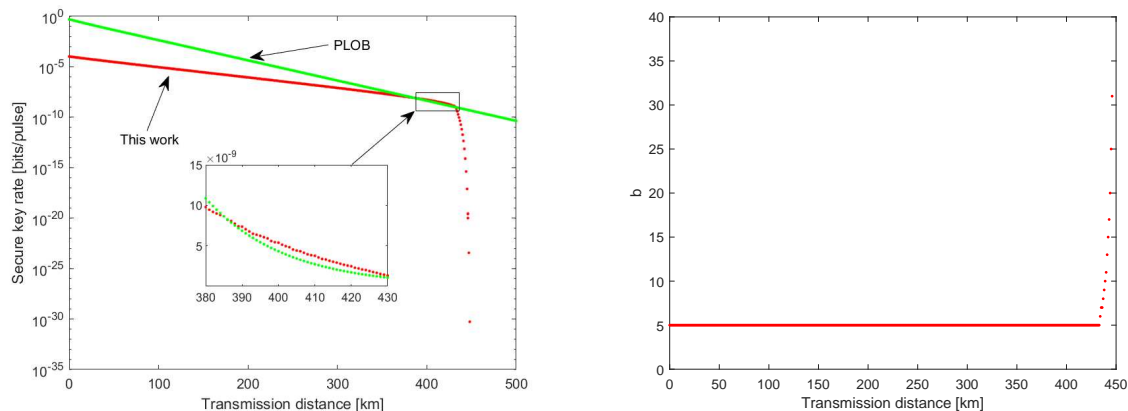
also be reached to 447 km.

From the simulation result, we find that our analysis method can generate positive secure key even if the loss-independent misalignment error is arbitrarily close to 0.5, the reason for which is that $E_{\mu\mu}^{XX}$ and $E_{\mu\mu}^{YY}$ have no correlation with e_d in the security analysis model. This is quite different from the BB84-QKD system or the original MDI-QKD system, where all of the error rate in different bases will be increased close to 0.5 by increasing e_d close to 0.5. However, in a TF-QKD system, we can prove that the error rate $E_{\mu\mu}^{ZZ}$ will be increased close to 0.5 by increasing e_d close to 0.5, but the error rate $E_{\mu\mu}^{XX}$ and $E_{\mu\mu}^{YY}$ will be unchanged. By applying the AD method with $b > 1$, the error rate $E_{uu}^{ZZ} = \frac{E_{uu}^{ZZb}}{E_{uu}^{ZZb} + (1 - E_{uu}^{ZZ})^b}$



(a) The relationship between the transmission distance and the secure key rate, the blue line is the secret key rate given by [19], the red line is the secure key rate given by this work, and the green line is the PLOB bound. (b) The relationship between the transmission distance and the optimal b values. From 0 km to 414 km, the optimal b value is 3.

FIG. 3. Results of TF-QKD protocol with $e_d = 0.3$.



(a) The relationship between the transmission distance and the secure key rate, the red line is the secure key rate given by this work, and the green line is the PLOB bound. (b) The relationship between the transmission distance and the optimal b values. From 0 km to 433 km, the optimal b value is 5.

FIG. 4. Results of TF-QKD protocol with $e_d = 0.41$.

will be smaller than $E_{\mu\mu}^{ZZ}$ at the cost of increasing $\tilde{\lambda}_0$ and $\tilde{\lambda}_1$. Thus, if b is large enough, we can also generate positive secure key rate R_{TF} even if the loss-independent misalignment error e_d is arbitrarily close to 0.5.

V. DISCUSSION

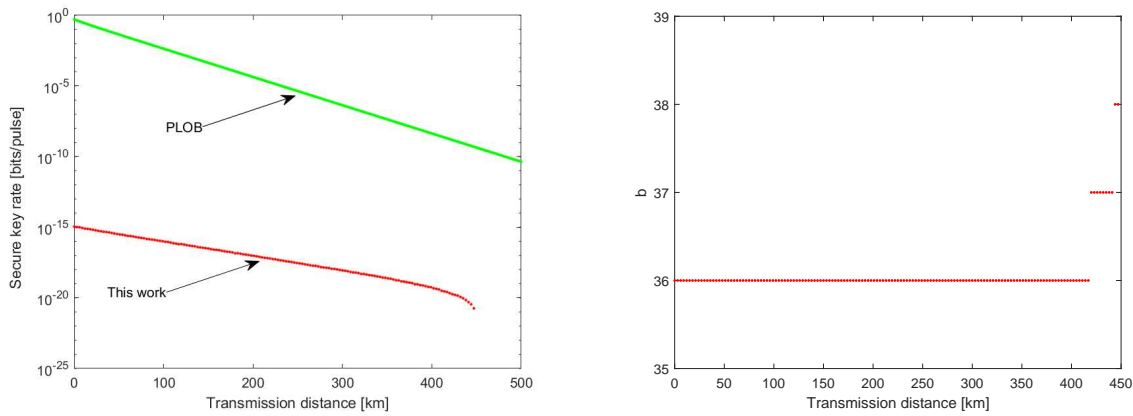
In a practical TF-QKD system, by combining the AD method with the information-theoretical security analysis method, we prove that both of the maximal transmission distance and the secure key rate can be sharply improved. More surprisingly, the numerical simulation result demonstrates that TF-QKD can generate positive secure key even if the loss-independent misalignment error is arbitrarily close to 50%, thus our analysis method

can significantly improve the performance of a practical TF-QKD system. In the future research, it will be interesting to experimentally realize the AD method in a practical TF-QKD system, especially with a high loss-independent misalignment error.

Since the AD method only modify the classical post-processing step, we can simply analyze the finite key length with the existed method. More precisely, based on the quantum asymptotic equipartition property [42], the leftover hash lemma [43] and the Chernoff bound [19, 44], the statistical fluctuation of the bit error rate and the secure key rate in finite-key length can be efficiently analyzed in the future research.

Code availability

Source codes of the plots are available from the corre-



(a) The relationship between the transmission distance and the secure key rate, the red line is the secure key rate given by this work, and the green line is the PLOB bound. (b) The relationship between the transmission distance and the optimal b values. From 0 km to 417 km, the optimal b value is 36.

FIG. 5. Results of TF-QKD protocol with $e_d = 0.49$.

sponding authors on request.

Data availability

The data that support the findings of this study are available from the corresponding authors on request.

Acknowledgements

The authors would like to thank Zhen-Qiang Yin, Shuang Wang and Guan-Jie Fan-Yuan for helpful discussions. This work is supported by National Key Research and Development Program of China (Grant No. 2020YFA0309702), NSAF (Grant No. U2130205), National Natural Science Foundation of China (Grant No.

11725524), Natural Science Foundation of Henan (Grant No. 202300410532) and China Postdoctoral Science Foundation (Grant Nos. 2019T120446, 2018M642281).

Author Contributions

Hong-Wei Li and Qing-Yu Cai conceived the project. Hong-Wei Li, Chun-Mei Zhang and Rui-Qiang Wang performed the calculation and analysis. Hong-Wei Li wrote the paper.

Competing Financial Interests

The authors declare no competing financial interests.

-
- [1] C. H. Bennett and G. Brassard, Quantum cryptography: public key distribution and coin tossing, in *Conf. on Computers, Systems and Signal Processing* (Bangalore, 1984) p. 175.
- [2] H.-K. Lo and H. F. Chau, Unconditional security of quantum key distribution over arbitrarily long distances, *Science* **283**, 2050 (1999).
- [3] P. W. Shor and J. Preskill, Simple proof of security of the bb84 quantum key distribution protocol, *Physical Review Letters* **85**, 441 (2000).
- [4] R. Renner, Security of quantum key distribution, *International Journal of Quantum Information* **6**, 1 (2008).
- [5] V. Scarani, H. Bechmann-Pasquinucci, N. J. Cerf, M. Dušek, N. Lütkenhaus, and M. Peev, The security of practical quantum key distribution, *Reviews of Modern Physics* **81**, 1301 (2009).
- [6] H.-W. Li, S. Wang, J.-Z. Huang, W. Chen, Z.-Q. Yin, F.-Y. Li, Z. Zhou, D. Liu, Y. Zhang, G.-C. Guo, *et al.*, Attacking a practical quantum-key-distribution system with wavelength-dependent beam-splitter and multiwavelength sources, *Physical Review A* **84**, 062308 (2011).
- [7] L. Lydersen, C. Wiechers, C. Wittmann, D. Elser, J. Skaar, and V. Makarov, Hacking commercial quantum cryptography systems by tailored bright illumination, *Nature Photonics* **4**, 686 (2010).
- [8] H.-W. Li, Z.-M. Xu, and Q.-Y. Cai, Small imperfect randomness restricts security of quantum key distribution, *Physical Review A* **98**, 062325 (2018).
- [9] S. L. Braunstein and S. Pirandola, Side-channel-free quantum key distribution, *Physical Review Letters* **108**, 130502 (2012).
- [10] H.-K. Lo, M. Curty, and B. Qi, Measurement-device-independent quantum key distribution, *Physical Review Letters* **108**, 130503 (2012).
- [11] L.-C. Kwek, L. Cao, W. Luo, Y. Wang, S. Sun, X. Wang, and A. Q. Liu, Chip-based quantum key distribution, *AAPPS Bulletin* **31**, 1 (2021).
- [12] S. Pirandola, R. Laurenza, C. Ottaviani, and L. Banchi, Fundamental limits of repeaterless quantum communications, *Nature Communications* **8**, 1 (2017).
- [13] M. Lucamarini, Z. L. Yuan, J. F. Dynes, and A. J.

- Shields, Overcoming the rate–distance limit of quantum key distribution without quantum repeaters, *Nature* **557**, 400 (2018).
- [14] X. Ma, P. Zeng, and H. Zhou, Phase-matching quantum key distribution, *Physical Review X* **8**, 031043 (2018).
- [15] X.-B. Wang, Z.-W. Yu, and X.-L. Hu, Twin-field quantum key distribution with large misalignment error, *Physical Review A* **98**, 062323 (2018).
- [16] C. Cui, Z.-Q. Yin, R. Wang, W. Chen, S. Wang, G.-C. Guo, and Z.-F. Han, Twin-field quantum key distribution without phase postselection, *Physical Review Applied* **11**, 034053 (2019).
- [17] M. Curty, K. Azuma, and H.-K. Lo, Simple security proof of twin-field type quantum key distribution protocol, *npj Quantum Information* **5**, 1 (2019).
- [18] J. Lin and N. Lütkenhaus, Simple security analysis of phase-matching measurement-device-independent quantum key distribution, *Physical Review A* **98**, 042332 (2018).
- [19] K. Maeda, T. Sasaki, and M. Koashi, Repeaterless quantum key distribution with efficient finite-key analysis overcoming the rate-distance limit, *Nature Communications* **10**, 1 (2019).
- [20] M. Minder, M. Pittaluga, G. Roberts, M. Lucamarini, J. Dynes, Z. Yuan, and A. Shields, Experimental quantum key distribution beyond the repeaterless secret key capacity, *Nature Photonics* **13**, 334 (2019).
- [21] X. Zhong, J. Hu, M. Curty, L. Qian, and H.-K. Lo, Proof-of-principle experimental demonstration of twin-field type quantum key distribution, *Physical Review Letters* **123**, 100506 (2019).
- [22] Y. Liu, Z.-W. Yu, W. Zhang, J.-Y. Guan, J.-P. Chen, C. Zhang, X.-L. Hu, H. Li, C. Jiang, J. Lin, *et al.*, Experimental twin-field quantum key distribution through sending or not sending, *Physical Review Letters* **123**, 100505 (2019).
- [23] S. Wang, D.-Y. He, Z.-Q. Yin, F.-Y. Lu, C.-H. Cui, W. Chen, Z. Zhou, G.-C. Guo, and Z.-F. Han, Beating the fundamental rate-distance limit in a proof-of-principle quantum key distribution system, *Physical Review X* **9**, 021046 (2019).
- [24] H. Liu, C. Jiang, H.-T. Zhu, M. Zou, Z.-W. Yu, X.-L. Hu, H. Xu, S. Ma, Z. Han, J.-P. Chen, *et al.*, Field test of twin-field quantum key distribution through sending-or-not-sending over 428 km, *Physical Review Letters* **126**, 250502 (2021).
- [25] J.-P. Chen, C. Zhang, Y. Liu, C. Jiang, W.-J. Zhang, Z.-Y. Han, S.-Z. Ma, X.-L. Hu, Y.-H. Li, H. Liu, *et al.*, Twin-field quantum key distribution over a 511 km optical fibre linking two distant metropolitan areas, *Nature Photonics* **15**, 570 (2021).
- [26] S. Wang, Z.-Q. Yin, D.-Y. He, W. Chen, R.-Q. Wang, P. Ye, Y. Zhou, G.-J. Fan-Yuan, F.-X. Wang, Y.-G. Zhu, *et al.*, Twin-field quantum key distribution over 830-km fibre, *Nature Photonics* , 1 (2022).
- [27] H.-L. Yin and Z.-B. Chen, Coherent-state-based twin-field quantum key distribution, *Scientific reports* **9**, 1 (2019).
- [28] M. Mastriani and S. S. Iyengar, Satellite quantum repeaters for a quantum internet, *Quantum Engineering* **2**, e55 (2020).
- [29] X.-M. Hu, C.-X. Huang, Y.-B. Sheng, L. Zhou, B.-H. Liu, Y. Guo, C. Zhang, W.-B. Xing, Y.-F. Huang, C.-F. Li, *et al.*, Long-distance entanglement purification for quantum communication, *Physical Review Letters* **126**, 010503 (2021).
- [30] G.-L. Long, D. Pan, Y.-B. Sheng, Q. Xue, J. Lu, and L. Hanzo, An evolutionary pathway for the quantum internet relying on secure classical repeaters, *arXiv preprint arXiv:2202.03619* (2022).
- [31] U. M. Maurer, Secret key agreement by public discussion from common information, *IEEE Transactions on Information Theory* **39**, 733 (1993).
- [32] B. Kraus, C. Branciard, and R. Renner, Security of quantum-key-distribution protocols using two-way classical communication or weak coherent pulses, *Physical Review A* **75**, 012316 (2007).
- [33] J. Bae and A. Acín, Key distillation from quantum channels using two-way communication protocols, *Physical Review A* **75**, 012334 (2007).
- [34] G. Murta, F. Rozpedek, J. Ribeiro, D. Elkouss, and S. Wehner, Key rates for quantum key distribution protocols with asymmetric noise, *Physical Review A* **101**, 062321 (2020).
- [35] E. Y.-Z. Tan, C. C.-W. Lim, and R. Renner, Advantage distillation for device-independent quantum key distribution, *Physical Review Letters* **124**, 020502 (2020).
- [36] D. Bruß, Optimal eavesdropping in quantum cryptography with six states, *Physical Review Letters* **81**, 3018 (1998).
- [37] W.-Y. Hwang, Quantum key distribution with high loss: toward global secure communication, *Physical Review Letters* **91**, 057901 (2003).
- [38] X.-B. Wang, Beating the photon-number-splitting attack in practical quantum cryptography, *Physical Review Letters* **94**, 230503 (2005).
- [39] H.-K. Lo, X. Ma, and K. Chen, Decoy state quantum key distribution, *Physical Review Letters* **94**, 230504 (2005).
- [40] H.-W. Li, C.-M. Zhang, M.-S. Jiang, and Q.-Y. Cai, Improving the performance of practical quantum key distribution with advantage distillation technology, (2021).
- [41] D. Gottesman and H.-K. Lo, Proof of security of quantum key distribution with two-way classical communications, *IEEE Transactions on Information Theory* **49**, 457 (2003).
- [42] M. Tomamichel, A framework for non-asymptotic quantum information theory, *arXiv preprint arXiv:1203.2142* (2012).
- [43] J. Radhakrishnan and A. Ta-Shma, Bounds for dispersers, extractors, and depth-two superconcentrators, *SIAM Journal on Discrete Mathematics* **13**, 2 (2000).
- [44] W. Hoeffding, Probability inequalities for sums of bounded random variables, *Journal of the American Statistical Association* **58**, 13 (1963).